First Experiences with Earthcloud, a Low-Cost, Cloud-Based IoT Seismic Alert System

Martin Klapez*†, Carlo Augusto Grazia*†, Simone Zennaro†, Matteo Cozzani†, Maurizio Casoni*
*Department of Engineering *Enzo Ferrari*,
University of Modena and Reggio Emilia,
via Vignolese 905, Modena, Italy.
{martin.klapez, carloaugusto.grazia, maurizio.casoni}@unimore.it
†Earthcloud Association
{martin.klapez, carloaugusto.grazia, simone.zennaro, matteo.cozzani}@earthcloud.it

***Abstract*—A Seismic Alert System (SAS) is one of the most important measures that can be taken to prevent and minimize earthquake damage. The role of a SAS is to detect as soon as possible an earthquake in progress and to then immediately alert about the impending earthquake waves all locations in danger. Clearly, to be of any utility, the communication of the alarm has to be transmitted way faster than the propagation speed of the earthquake waves. This paper presents the rationale, setup and first results of a deployed Earthcloud prototype, an experimental SAS designed to be low-cost, low-power, and cloud-based. Earthcloud is devised to alert locations that are not too close yet not too far from the earthquake epicenter, i.e., those that can benefit from an alarm received from a few seconds to tens of seconds earlier. The system has been designed to leverage existing Internet infrastructures in order to perform both computation and communication in the cloud, minimizing costs and maximizing communication speed and deployment ease. Data harvested by Earthcloud has been cross-referenced with data from the Italian National Institute of Geophysics and Volcanology and, although still in a prototype stage, the first results indicate that the system can correctly detect earthquakes.**

***Index Terms*—Cloud, Earthquake Warning System (EWS), IoT, Public Safety Network**

I. Introduction

A SAS, also called Earthquake Warning System (EWS) or Earthquake Early Warning system (EEW or EEWS), can effectively serve to briefly anticipate earthquakes for a subset of the locations interested by the event. Sites that reside on or very near the epicenter have unfortunately no way of being alerted in useful time. However, they can be the first to detect an earthquake, and they can subsequently react by triggering an alarm alerting farther places before destructive waves reach them. With such systems, due to the relatively fast propagation of earthquake waves, it is only possible to receive alerts in a timeframe that goes from a few seconds to tens of seconds before the strike. Nevertheless, they can potentially yield very significant benefits. If an earthquake occurs at night when people are usually sleeping, for instance, the primary risk for human health (primary in terms of the number of people affected) is represented by the possible collapse of buildings or parts of them. Potential victims usually wake up abruptly, most likely in a state of panic and with the risk of being overwhelmed by events. Risks for human health would be even higher if an earthquake occurs during the day when many people are working or traveling. Examples of these hazards, unfortunately, abound and can go from small injuries to large-scale nuclear disasters. For instance, derailment of trains on railroads and subways, vehicles on bridges and tunnels, dangerous machines and chemicals in work environments, suspended loads and work at heights in building sites, fires, and more, plus the collapse of buildings, as mentioned earlier. In addition to all of these, some risks involve machinery that may or may not affect human health, but that would inevitably cause economic damage. Receiving a seismic alert, even if only seconds before the arrival of destructive waves, can prevent human losses, injuries, and damage to machinery and infrastructures. For instance, it can trigger the enforcement of a previously approved emergency plan, that for people can consist in moving away from hazardous equipment, taking cover under desks or load-bearing structures, etc. Machinery, on the other hand, can be automatically slowed, shut down, and/or isolated, to prevent damage as well as to avoid the ignition of cascading threats, such as fires that can kindle in the aftermath of an earthquake.

This paper presents Earthcloud, an Internet of Things (IoT) SAS designed to be low-cost, low-power, and cloud-based. The system is composed of a series of devices that, when deployed, serve as sensors for ground movement. When variations are detected, data is sent to a centralized cloud-based database. The cloud system is responsible for analyzing data and, therefore, for distinguishing real earthquakes from false positives. If ground waves are confirmed, the system sends an alarm signal to registered users in the to-be-affected geographical area. The article is organized as follows. Section II pinpoints related work. Section III summarizes the necessary geological concepts. Section IV details the deployed prototype. Section V presents the outcomes of a month of recordings. Section **??** illustrates the next steps to evolve the prototype into a fully-fledged system. Section VI concludes the writing.

II. Related Work: an overview on SASs

The goal of this Section is not to be exhaustive; is it instead to present an indicative group of works from academia and industry, to form a representative overview of the options, to point the reader to relevant sources, and to highlight the main differences with our work.

In literature, one of the first works on SASs based on computer technology dates back to 1996 [1]. Authors designed a neural network and trained it with real data extracted from seismograms. Then, the neural network has been fed with other data from the same sources, and its outcomes have been studied. An actual system was not developed, but the algorithm was successful in the accurate estimation of hazard start, stop and duration time. The algorithm was able to generate a warning signal 0.3 seconds after detecting the first ground motion.

Earthcloud utilizes geophones as sensors (see Section IV), while the majority of prototypes reported in the literature that aim to be low-cost use MEMS (i.e., Micro Electro-Mechanical System) accelerometers for the same purpose. In [2], for instance, authors built a prototype where sensors are composed of accelerometers attached to Arduino microcontrollers. The control system is a LabVIEW software on a laptop that communicates with sensors through the ZigBee standard. A ZigBee antenna can theoretically have a range up to hundreds of meters but, generally, actual range is in the order of tens of meters. The latter applies to the system, as presented by the authors. With respect to Earthcloud, it is also moderately more complex to set up. From the paper, it is not clear whether the prototype has been deployed or not. Another work that leverages accelerometers and Arduino microcontrollers is presented in [3]. Instead of ZigBee, a GSM module is employed, and the system is tested against a vibration generator machine. The focus of the authors, however, is in this case on signal analysis. Earthcloud sensors are currently based on Raspberry Pi boards instead of on Arduinos. This has been a deliberate choice, as Raspberry Pis are more limited on the hardware side but more flexible on the software side. As an Earthcloud core concept is to leverage cloud services (see Section IV), the right choice was obvious.

Accelerometers embedded in smartphone have also been extensively used. For instance, authors in [4] test these sensors specifically for SASs applications and study how to separate false positives from real ground motion, although tests are performed against artificial data obtained with a shakeboard, and smartphones are positioned on horizontal flat surfaces for the entire duration of the experiments. Shakeboards are also employed to test prototypes designed to form an IEEE 802.11 (WiFi) Wireless Mesh Network [5], [6]. In these cases, however, authors focus specifically on the performance of wireless communications. They found that the sudden small-amplitude P-waves (see Section III) shaking can have a huge impact on those performance, especially with no or scarce Line Of Sight between transceivers. Accelerometers in smartphones have also been coupled with cloud elaboration before. Authors in [7] rely on 2G/3G/4G cellular technologies or IEEE 802.11 to pass data between devices and a cloud service. However, most of the paper is spent detailing the software development cycle of the proposed Android application, and very few information can be found about the effectiveness of the system.

Other works focus on unconventional systems. Authors in [8] use the same low-cost accelerometer sensors seen in other solutions. However, sensors transmit data to a computer that, in the event of an emergency, transforms the alarm signal in SMS form and then send it through cellular networks. Another workstation has been set up to receive those SMS and measure the elapsed time. Authors found that, although the delays varied, on average these exceeded the maximum tolerable delay for a SAS, and concluded that SMS is not a reliable platform for those means. An unorthodox sensor is presented in [9]. Authors propose to detect ground motions through the variations in read/write error rates of common electromechanical magnetic hard disks. The distributed system is designed in a P2P fashion. As in [7], the SAS would require substantial user collaboration to work correctly. Alternatively, although vendors would probably oppose such a choice for security and privacy reasons, operating systems might be modified to perform those SAS tasks in the background, without the users' consent. Anyway, the system may become weak in the long term, as magnetic hard drives are replaced by faster solid-state storage devices.

About systems that rely on users collaboration through software deployed on common devices, the Earthquake Network Project [10] is one of the best examples, claiming 4 million downloads of its Android application, 750000 active users, and more than a 1000 early warnings sent. While the analysis of data coming from the network of smartphones is not trivial, statistical approaches are being studied to improve the system [11].

An example of SASs from industry is ShakeAlarm [12], developed by Weir-Jones Engineering Consultants, a system that detects P-waves (see Section III) and claims to be able to determine in less than 0.5 seconds if following waves will be dangerous. ShakeAlarm is deployed in some regions of Canada and of the USA. There are also SASs developed by institutions and deployed on a large scale. In Japan, the Japan Meteorological Agency operates an EWS [13] mainly formed by about 300 single-function and multi-purpose seismometers; the latter are equipped with satellite mobile phone communication capability for backup purposes and a power supply that can keep the whole system operational for about 72 hours in the event of power failure. The Japanese EWS fetches data also from seismometers managed by universities, by the National Research Institute for Earth Science and Disaster Resilience, and by the Japan Agency for Marine-Earth Science and Technology. Taiwan also has a nationwide SAS [14], while Mexico has a partial EWS called SASMEX that comprises the SAS of Mexico City, in continuous operation since 1991, and the SAS of Oaxaca City that started its services in 2003. In the United States, the west coast is currently covered by an experimental system called ShakeAlert [15], [16].

III. Key Geological Concepts

Earthquakes are generated in an area called the nucleation zone. Most of the times, this area is located inside the seismo-

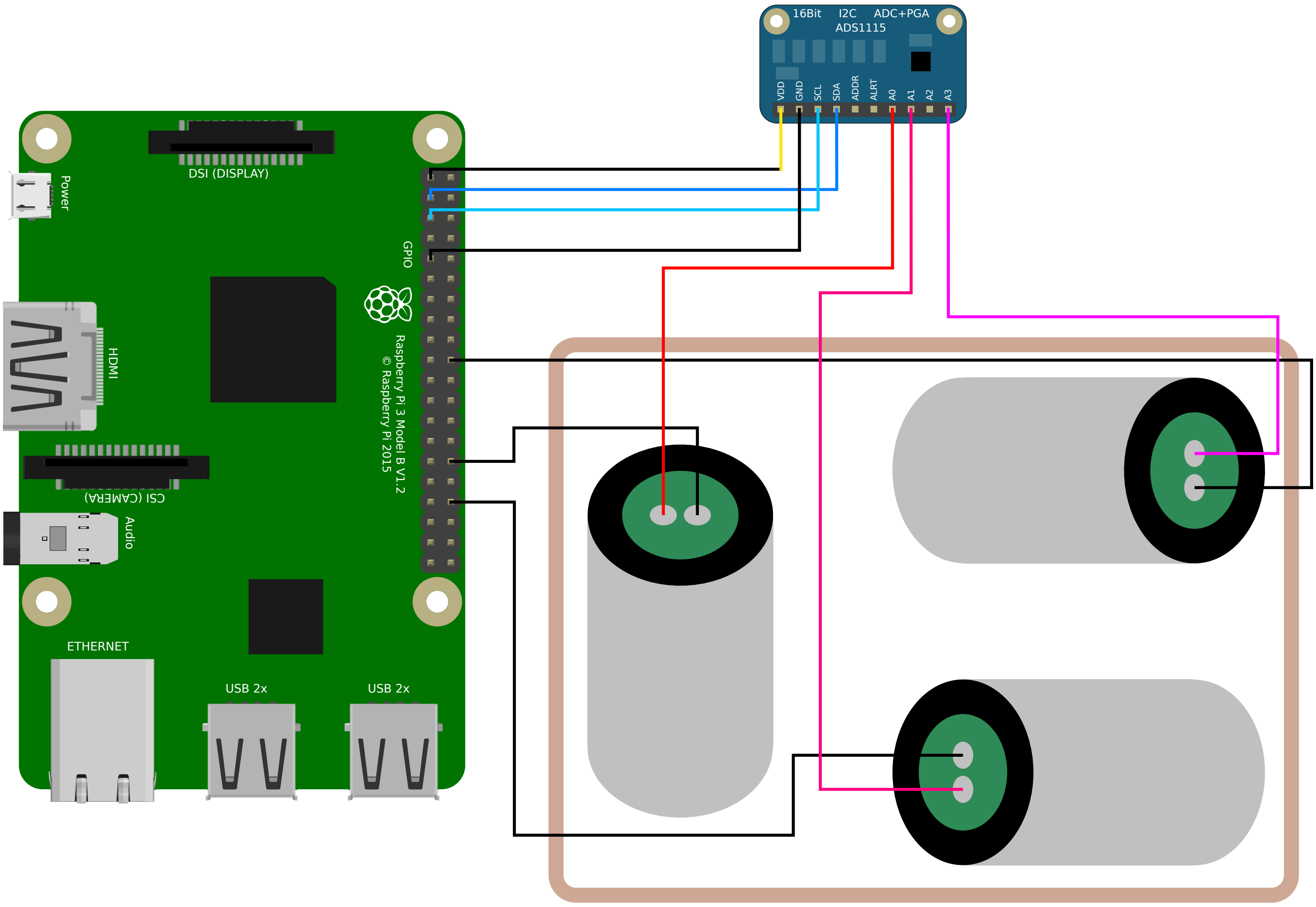

Fig. 1: An Earthcloud Sensor Subsystem

genic layer, that is the part of the Earth's crust with a depth ranging from 5 to 30 km. In the nucleation zone, multiple types of waves are generated, with different characteristics based on destructive potential and speed.

These waves come in two arrivals. The time between the two is the opportunity to detect, confirm the earthquake and send an alarm signal. Each of these two arrivals consists of many individual elastic waves that have traveled from the epicenter to recombine at the recording site as a function of their respective velocities, focal distances, and propagation paths. Waves belong to two types: body waves and surface waves.

The first arrival is composed by the fastest of body waves, the P-waves (from Latin *prima unda*, i.e., primary waves). These are compressional or longitudinal and shake the ground in the direction of their propagation using compression or rarefaction, while their speed is between 4 and 8 km/sec. P-waves are usually not destructive.

Body waves and surface waves may compose the second arrival. They often produce both horizontal and vertical ground motion and their peak velocities, peak accelerations, and duration in time may cause significant damage to structures.

The body waves in the second arrival are called S-waves (from Latin *secunda unda*, i.e., secondary waves); they shake the ground in a direction that is perpendicular to the direction of propagation, while their speed is about 60% to that of the respective P-waves [2]. S-waves can be destructive in up to several kilometers from the epicenter due to the phenomenon of seismic amplification, linked to the local geology and morphology.

Surface waves are categorized into two types, called Love and Rayleigh, from the name of the scientists that modeled them. They are formed by constructive interference between P-waves and S-waves, and they are the most dangerous. Love waves travel slower than both P-waves and S-waves; Rayleigh waves are the slowest. However, while they are slower, surface waves decade much less with the distance than body waves, as they mainly travel on one axis instead of three. The Earth's crust where they travel acts as a waveguide that provides little attenuation loss. In big earthquakes, they may circumnavigate Earth several times before being completely dissipated. In general, surface waves cause more movement than body waves. In addition, the interaction among them as they propagate can produce considerable amplification of ground motion near the surface, a phenomenon called the free surface effect that occurs when upgoing and downgoing

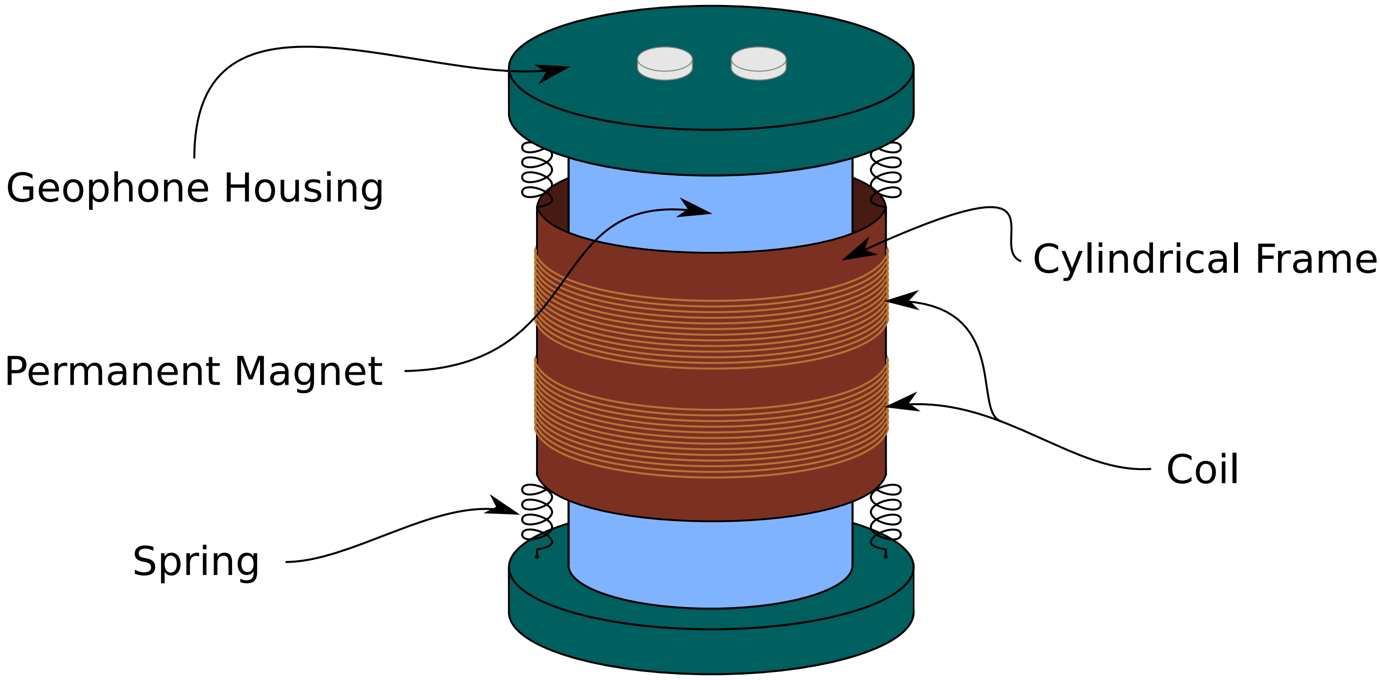

Fig. 2: Inside an Earthcloud Geophone

reflected waves are in phase and of considerably greater wavelength than the thickness of the crust.

IV. Prototype Set up

The following Subsections detail the first prototype of Earthcloud by presenting the two main parts of the system, i.e., sensor systems and cloud services, separately.

A. Sensors: Why Geophones?

An Earthcloud sensor system is composed of three elements: a Raspberry PI 3 Model B V1.2, an analog-digital converter (Adafruit ADS1115), and a set of 4.5 Hz geophones enclosed in a firm structure. Figure 1 depicts the system and details the wired connections among elements. Size proportions are realistic. Raspberry Pis mount a Linux distribution as operating system; specifically, they mount Raspbian Stretch 9.4 with Linux kernel version 4.14-34 (4.14.34-v7+). The Earthcloud sensor elements are the geophones. They usually sit in between accelerometers and seismometers in function and price, the latter being the most accurate, delicate and expensive system. As Earthcloud aims to be low-cost, we chose geophones over accelerometers as they should also allow the detection of relatively distant earthquakes.

A typical geophone has one working axis and has the function to convert ground movement that has the same direction of the working axis into voltage. Therefore, any voltage deviation from the baseline is data. A typical geophone consists of a housing and, inside, of a mass suspended by means of mechanical springs. The spring-mass system has a resonance frequency, also called natural frequency, in the working axis of the geophone. Conceptually, when the sensor moves, if the velocity produces a frequency that is lower than the natural, both housing and mass move. If the generated frequency is higher, only the housing moves and the mass tends to hold its position.

In modern geophones, like those used by Earthcloud, the mass is formed by a cylindrical frame in which, externally, two coils are attached so as to surround the cylinder. The double coil allows reducing data distortion. The cylinder and coil assembly are usually supported by springs, directly connected to the geophone housing. Inside the cylinder frame, there is a permanent magnet also directly attached to the housing, that does not move. Figure 2 illustrates a typical geophone of this kind.

Therefore, if the movement frequency is lower than the natural, there is conceptually no internal movement at all if considering the relationship between coils and magnet; i.e., the variation in the position of the coils with respect to that of the magnet is zero. If the frequency exceeds the natural, coils tend to maintain their position while the magnet moves with the housing; therefore, there is a shift in location between coils and magnet. As the coils are in the field of the magnet, this shift produces a variation in voltage that is proportional to the movement velocity. If the geophone is fixed to the ground, its response is (if above natural frequency) proportional to ground velocity. For comparison, MEMS accelerometers respond to ground acceleration.

Geophones also have what is called a spurious frequency, usually due to the small movements that the mechanical springs can have in directions perpendicular to the working axis of the sensor. These springs, in fact, are designed to move linearly in the working axis but also to have the possibility of small movements in the plane perpendicular to the working

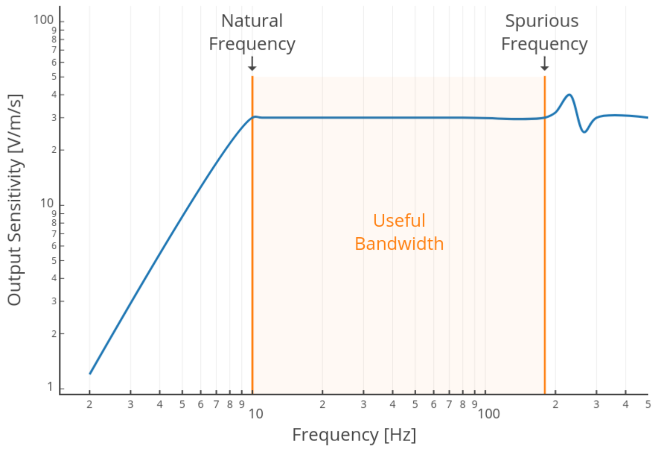

Fig. 3: A transfer function for a typical 10 Hz geophone, with ~60% damping and 180 Hz spurious frequency

Name	EG-4.5-II
Natural frequency	4.5 ± 10% Hz
Damping	0.6 ± 5%
Coil resistance	375 ± 5% 1 Ω
Open circuit sensitivity (V/m/s)	28.8 ± 5%
Harmonic distortion	$\leq$ 0.2%
Typical spurious Frequency	$\geq$ 150 Hz
Moving mass	11.3 g
Max. coil excursion p-p	4 mm
Element diameter	25.4 mm
Element height	36 mm
Element weight	86 g
Operating Temperature	-40°C to +100°C

TABLE I: Technical specifications of the geophones used

axis. Motion in this plane, either transverse or rotational, is essential to allow freedom of mobility in the working axis for the cylinder and coil assembly. As there is a resonance frequency in the working axis, called natural frequency, there is also a resonance frequency in the axis perpendicular to the former, that is called spurious frequency (actually, there are spurious frequenc*ies*, the lowest is taken as the spurious). The springs are, of course, very stiff in the direction perpendicular to their working axis; hence, the high-frequency nature of the spurious resonance [17]. As shown in Figure 3, the natural frequency represents the lower bound of the usable bandwidth, while the spurious frequency the upper bound. Therefore, the two frequencies together determine the useful frequency range of the sensor. For all frequencies in this bandwidth, the output sensitivity (i.e., the smallest variation in voltage that can be measured by the sensor) remains approximately constant.

As it can be seen from Figure 3, the actual response of a geophone is not an on-off boolean function. The mass still moves below the resonance frequency, but output resolution (i.e., the smallest variation in space that can be measured by the sensor) drops fast (output resolution is calculated by dividing sensitivity over noise, S/N). Inverse filtering can compensate by flattening the response below the natural frequency of the geophone, but it is only useful if there is an adequate signal-to-noise ratio. On the other hand, for frequencies higher than the spurious one, springs introduce additional resonances that generate noise and therefore lower resolution. Inconsistencies in materials and manufacturing processes have a substantial effect on the determination of the spurious frequency, hence its common specification as $SF \geq x$, which indicates that the actual frequency band in which spurious resonance will occur may be x or a $y > x$.

Geophones usually maintain signal digitization as a separate process, as the analog output is generated in the sensor first and then is sent to an external digitizer. For comparison, MEMS accelerometers derive their feedback from within the digitizing process instead. In general, accelerometers have lower noise at high frequencies, while geophones have lower noise at low frequencies. The signal itself actually degrades slower with MEMS accelerometers, usually around a 6-dB as the frequency halves. For comparison, the same figure for standard geophones is about 12-dB [18]. This should make the former sensors good candidates for low-frequency recording; if the signal is strong, this is indeed the case. The problem with MEMS accelerometers is the intrinsically high self-noise which makes them unsuitable for accurate low-frequency signals detection. Table I lists the technical specifications of the geophones currently used by Earthcloud. As shown in Figure 1, an Earthcloud sensor includes three geophones for three different axes that permit to gather data in a 3D domain. The sensors are enclosed in a firm wooden structure.

B. *Cloud Services*

Figure 4 shows the overall architecture of Earthcloud together with the composition of cloud services. At the moment, the latter are based on the Amazon AWS platform, in which Earthcloud services mainly operate from Ireland, EU.

IoT is a paradigm based on the connection between devices in the physical world, often sensors and data-gathering devices, and the Internet. Each Earthcloud sensor generates data that, if considered suspicious, may trigger a first alarm that travels from the sensor itself to registered entities. Data generated by the Earthcloud sensors are encapsulated in MQTT messages initially fed to AWS IoT, which preprocess and route them through Amazon Kinesis. Sensor data is small in size but can be continuously generated, from, potentially, thousands of sources. For Earthcloud, Kinesis has two functions: processing data, and delivering it, both in real-time. Clearly, the *real-time* part (depicted in Figure 4 with a light red background) is critical for Earthcloud. If the system considers the incoming data suspicious, it performs further processing on that data. If an earthquake is suspected, an alarm signal is sent to registered entities, that can be the second or the first in case sensor devices did not trigger one. Kinesis also acts as a bridge between AWS IoT, the data entry-point, and Amazon S3, the data endpoint. If needed, data can be converted into

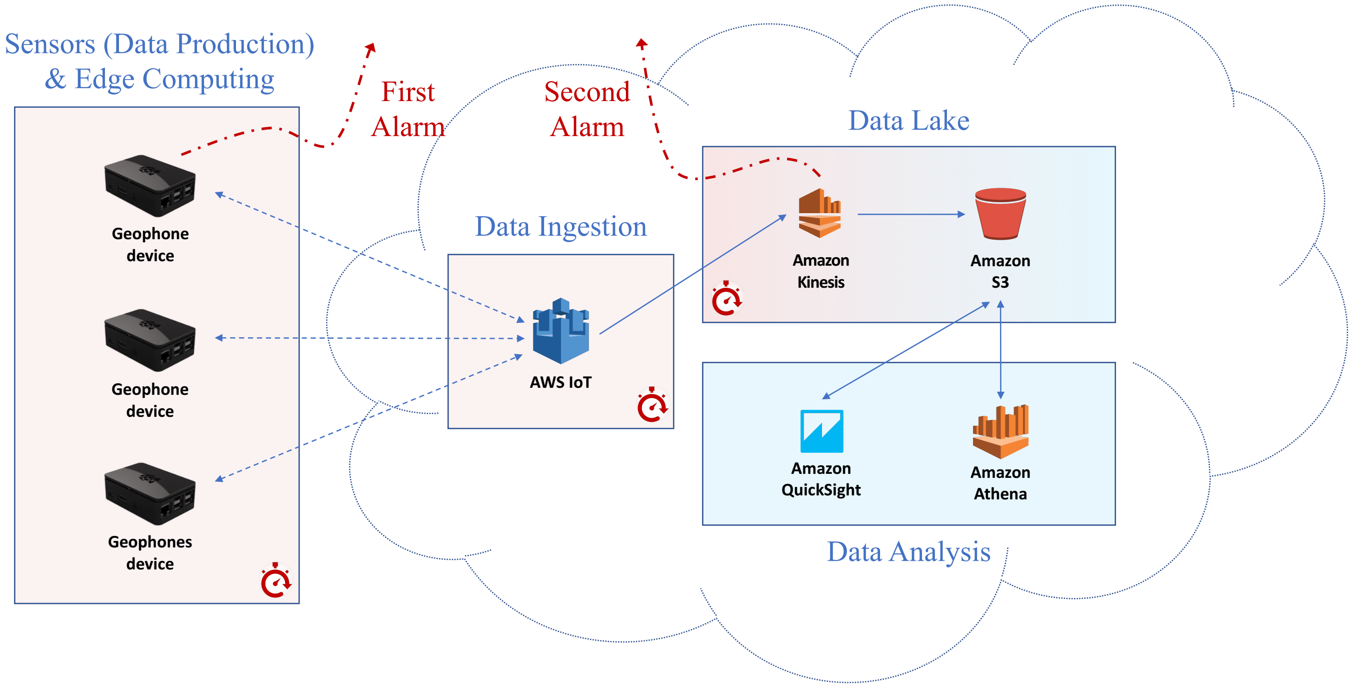

Fig. 4: Earthcloud Architecture

different formats before leaving the bridge. Amazon S3 is a data storage, well integrated with the other services from the same vendor.

Data in S3 can be then further analyzed, manually and automatically. Amazon Athena allows querying S3 data through regular SQL (S3 data are stored as objects, not as SQL rows), while Amazon QuickSight, or other solutions, ease or perform data analysis. All the passages from Amazon S3 forward are regarded as batch processing (depicted in Figure 4 with a light blue background); more sophisticated analyses can be performed, but it can take anywhere from few seconds to few minutes to obtain the results. Although it is in the works, we do not have a system based on machine learning implemented at this stage. However, as the data set grows, all relevant data collectible from S3 becomes more valuable to train a suitable neural network adequately.

C. Considerations on Redundancy

Cloud services are provided with already built-in redundancy features, at least as long as they are deployed on premises of established vendors. However, as strong earthquakes are likely to disrupt infrastructures [19], [20], [21], [22], [23], we believe redundancy should be introduced to sensor devices too. As we used flexible, low-cost, and low-power devices, it should be feasible to power them with small rechargeable batteries as well as to enable on them multiple connection channels, all while retaining financial convenience.

V. Outcomes from a Month of Recordings

The first prototype of Earthcloud consists of the cloud system (in beta) and three devices. These have been deployed in Modena, an Italian city in the Emilia-Romagna region, a mid-north area of Italy, EU, classified as a moderate-to-high seismic zone according to the 1999 Global Seismic Hazard Map [24]. In 2012, a seismic swarm struck Modena's area with intense earthquakes [25]. The first strong earthquake was registered on May 20, 2012, at 02:03:52 UTC (04:03:52 local time, i.e., at night). It had a 5.9 Richter Magnitude (M_L, for Local Magnitude) and a hypocenter located 6.3 km underground. Other subsequent earthquakes followed, two with 5.1 M_L. Seven people died, 50 were injured, and 5000 lost their houses, while many historical buildings collapsed, together with several farms and factories. Consequential to the disaster, soil liquefaction also caused collapses of recently-built structures. On May 29, 2012, a second strong earthquake hit the same region with a 5.8 ML and a 10.2 km-deep hypocenter, at 07:00:03 UTC (09:00:03 local time, i.e., in the morning). Other subsequent earthquakes followed, among which one with 5.3 M_L and another with 5.1 M_L. Consistently with what exposed in Section I, damages were more significant. 20 people died, 350 were injured, and 10000 more lost their houses. Among the aftershocks that followed, on June 3, 2012, another one with 5.1 M_L hit the area. There were building damage and collapse, but no casualties. The two strongest earthquakes were also felt in nearby European countries, in particular in southeast France, Switzerland, south Germany, Austria, Slovenia, and Croatia. Damages were classified on the Mercalli scale (EMS-98), that classifies earthquake damages instead of its released energy, with a value of $8/12$.

Two sensors have been initially installed on June 19, 2018, at the Department of Engineering Enzo Ferrari of the Uni-

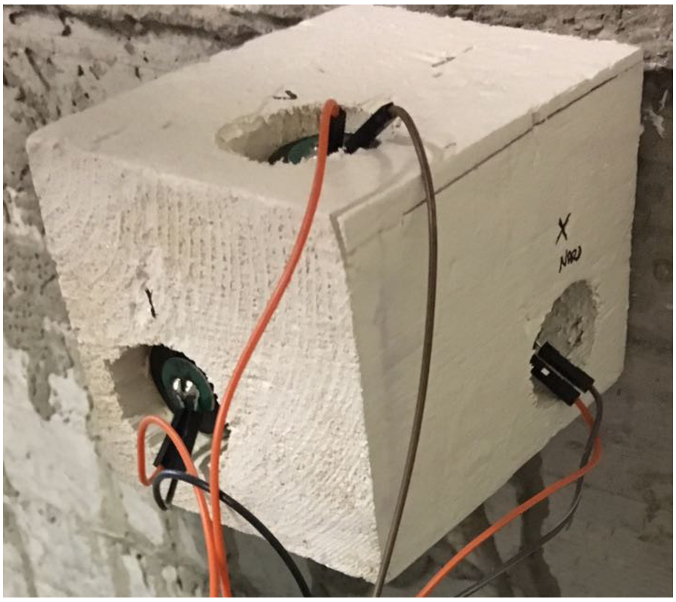

Fig. 5: Geophone Housing

versity of Modena and Reggio Emilia, inside a temperature-controlled server room. Devices are connected to the Internet through Ethernet cables, directly attached to the department switches for minimum latency, and are powered through electrical outlets. The geophone housings have been firmly mounted directly on walls concrete, with an industrial-grade wood-concrete glue. One has been installed on a load-bearing wall, while the other on a wall next to the room door, which is opened and closed very infrequently. The intent was to have two sensors in the same place but with one more sensitive to false positives. A week later, a third sensor has been deployed in a storage room belonging to a dismissed industrial building, located in a different area of the same city. The geophone housing was mounted on a load-bearing wall. This device was also connected to the Internet through an Ethernet cable, but with the difference of the latter being attached to a commercial off-the-shelf router manufactured for domestic purposes. Power was again provided by an electrical wall outlet. For the first prototype, unrefined ad-hoc containers for geophones have been built by creating several rectangular prisms of approximately the same size from solid wood. Three holes to house the geophones have been drilled in each container, two for horizontal axes and one for the vertical axis, as in Figure 5. The holes allow for very limited movement of the geophones inside the housing, around 1 mm. As data analysis gets refined, more sophisticated housings will be created, in order to further minimize geophone allowances inside their containers or cancel them altogether.

On July 1, 2018, a low-power earthquake of Magnitude 3.6 on the Richter scale struck the region at 07:32:16 UTC (09:32:16 local time), with an hypocenter 14 km deep and epicenter 59.11 km (36.73 mi) and 59.69 km (37.09 mi) from the first two devices and the third one, respectively, in a straight line. The farther distance where the earthquake was perceived, instead, has been reported to be approximately 58 km in a straight line from the epicenter. High frequencies attenuate faster and, as the natural frequency of the geophones is relatively low at 4.5 Hz, there was the possibility that sensors would have registered useful data, even if people next to them noticed nothing. First alarm functionalities (see Figure 4) were not deployed yet. Data harvested by Earthcloud on July 1, 2018, has therefore been batch processed and cross-referenced with data of the same day from the Italian National Institute of Geophysics and Volcanology (INGV), that in turn sources data from the Italian National Seismic Network and other local, regional and national networks belonging to other national or international institutions.

From cloud data gathered through Athena, it was confirmed that the two co-located devices detected the arrival of P-waves on all three directional axes, with peak values of $|0.5|\,mV$, at 07:32:31 UTC (09:32:31 local time) of the device clocks. The third device did not produce useful data, as we did not manage to differentiate earthquake waves from background noise. Several reasons may account for this noise in data; most likely, either the device was misconfigured, its assembly on the wall poorly performed, or it had some component (e.g., the analog-to-digital converter) failure. Considering a straight line distance of $59.110\,km$ at earth level and a hypocenter with a $14.000\,km$ depth, an approximation of the actual source point of the earthquake can be calculated as the hypotenuse of the right triangle formed through the previous figures, that is equal to $60.745\,km$. Counting a time difference of $15.000\,s$, and assuming that device clocks were synchronized with INGV time, the resulting P-wave average velocity between the source and the detection point would be equal to $4.050\,km/h$. This figure is slightly higher than the lower end of the often-reported speed interval for P-waves of $[4-8]\,km/h$. Actually, as reported in [26], P-waves can travel from anywhere between 300 and 6500 m/s, depending on the terrain composition. Considering the presence of significant marshy deposits in the region (Modena, in the past, was a very swampy terrain), which can hamper wave propagation, it is plausible to expect wave propagation velocity attenuations when comparing it to average values. Furthermore, no other relevant data could be extracted from Athena in a slightly larger timeframe. Therefore, the detection was considered positive.

At 07:32:38 UTC (09:32:38 local time), the *secunda unda* was identified. Earthcloud detected S-waves until 07:32:40 UTC (09:32:40 local time), through data with peak values of $|1.125|\,mV$ from the co-located devices. Detection started at second 38 and ended at second 40, resulting in a traveling time of $22.000\,s$ and $24.000\,s$, respectively, that give average velocities of $2.761\,km/h$ and $2.531\,km/h$, each, calculated following the same logic used for P-waves. The mean value between the two results in $2.646\,km/h$. The latter is $65.333\,\%$ of the P-wave average velocity, an amount that is consistent to the typical approximate figure of $60\,\%$ that relate S-wave speed with the preceding P-wave speed, when considering the same direction and the same traversed materials. As a consequence, the detection was deemed to be positive.

Acknowledgments

The authors would like to express their gratitude to both the Department of Engineering Enzo Ferrari and the Ovestlab center (http://ovestlab.it) together with its head, Silvia Tagliazucchi, for allowing us to use their respective premises and resources for our devices without charge.

VI. Conclusions

This article presented the first prototype of Earthcloud, a SAS designed to be low-cost, low-power and cloud-based. Three sensor devices have been deployed in a moderate-to-high Italian seismic zone that witnessed significant earthquakes in recent years, while an initial cloud service has been developed and configured. Soon after the system went operative, a low-power yet noticeable earthquake hit with a 14 km-deep hypocenter and an epicenter located approximately 60 km in a straight line from where sensor devices were deployed. One out of the three sensors failed to isolate seismic waves but generated noise instead, while the other two succeeded in sending relevant data to the cloud. Earthcloud detected a possible earthquake and, as a consequence, cloud data have been analyzed in the aftermath. Results indicates a significant correlation between the elaborated material and the seismic data published by the relevant national authority, yielding a promising outcome.

References

[1] R. R. Leach and F. U. Dowla, "Earthquake early warning system using real-time signal processing," in *Neural Networks for Signal Processing VI. Proceedings of the 1996 IEEE Signal Processing Society Workshop*, Sep 1996, pp. 463–472.

[2] R. Hoque, S. Hassan, M. A. Sadaf, A. Galib, and T. F. Karim, "Earthquake monitoring and warning system," in *2015 International Conference on Advances in Electrical Engineering (ICAEE)*, Dec 2015, pp. 109–112.

[3] Y. Sherki, N. Gaikwad, J. Chandle, and A. Kulkarni, "Design of real time sensor system for detection and processing of seismic waves for earthquake early warning system," in *2015 International Conference on Power and Advanced Control Engineering (ICPACE)*, Aug 2015, pp. 285–289.

[4] T. Uga, T. Nagaosa, and D. Kawashima, "An emergency earthquake warning system using mobile terminals with a built-in accelerometer," in *2012 12th International Conference on ITS Telecommunications*, Nov 2012, pp. 837–842.

[5] J. Nachtigall, A. Zubow, R. Sombrutzki, and M. Picozzi, "The Challenges of Using Wireless Mesh Networks for Earthquake Early Warning Systems," in *2009 Second International Conference on Advances in Mesh Networks*, June 2009, pp. 155–162.

[6] J. Nachtigall and J. P. Redlich, "Wireless Alarming and Routing Protocol for Earthquake Early Warning Systems," in *2011 4th IFIP International Conference on New Technologies, Mobility and Security*, Feb 2011, pp. 1–6.

[7] A. Heryana, E. Nugraheni, B. Kusumo, A. F. Rojie, and B. Setiadi, "Applying agile methods in designing an earthquake and landslide early warning system application for Android," in *2017 International Conference on Computer, Control, Informatics and its Applications (IC3INA)*, Oct 2017, pp. 80–84.

[8] E. Shayo, A. Mwambela, and S. Kawambwa, "Evaluating Quality of Service for Short Message Service as a Platform to Transmit Seismic Data in Earthquake Early Warning System," in *2018 IST-Africa Week Conference (IST-Africa)*, May 2018, pp. Page 1 of 6–Page 6 of 6.

[9] E. Heindl, "Peer-to-peer (P2P) earthquake warning system based on collaborative sensing," in *2009 3rd IEEE International Conference on Digital Ecosystems and Technologies*, June 2009, pp. 174–176.

[10] F. Finazzi, "The Earthquake Network Project: Toward a Crowdsourced Smartphone-Based Earthquake Early Warning SystemThe Earthquake Network Project: Toward a Crowdsourced Smartphone-Based Earthquake Early Warning System," *Bulletin of the Seismological Society of America*, vol. 106, no. 3, p. 1088, 2016. [Online]. Available: http://dx.doi.org/10.1785/0120150354

[11] F. Finazzi and A. Fassò, "A statistical approach to crowdsourced smartphone-based earthquake early warning systems," *Stochastic Environmental Research and Risk Assessment*, vol. 31, no. 7, pp. 1649–1658, Sep 2017. [Online]. Available: https://doi.org/10.1007/s00477-016-1240-8

[12] A. Zaicenco, S. Huffman, and I. Weir-Jones, "Seismic P-wave Polarization in the Context of On-site Early Warning System," in *International Conferences on Recent Advances in Geotechnical Earthquake Engineering and Soil Dynamics*, no. 13, May 2010, Accessed on July 25, 2018. [Online]. Available: http://scholarsmine.mst.edu/icrageesd/05icrageesd/session03/13/

[13] "Earthquake and Tsunamis - Disaster prevention and mitigation efforts," Japan Metereological Agency, JMA, March 2018, Accessed on July 25, 2018. [Online]. Available: http://www.jma.go.jp/jma/kishou/books/jishintsunami/en/jishintsunami_en.pdf

[14] Y.-M. Wu, N.-C. Hsiao, T.-L. Chin, D.-Y. Chen, Y.-T. Chan, and K.-S. Wang, *Earthquake Early Warning System in Taiwan*. Berlin, Heidelberg: Springer Berlin Heidelberg, 2013, pp. 1–12. [Online]. Available: https://doi.org/10.1007/978-3-642-36197-5_99-1

[15] E. R. Burkett, D. D. Given, , and L. M. Jones, "ShakeAlert - An earthquake early warning system for the United States west coast," U.S. Geological Survey Open-File Report 2014–1097, USGS Earthquake Science Center, February 2017.

[16] D. Given, E. Cochran, T. Heaton, E. Hauksson, R. Allen, P. Hellweg, J. Vidale, and P. Bodin, "Technical Implementation Plan for the ShakeAlert Production System - An Earthquake Early Warning System for the West Coast of the United States," U.S. Geological Survey Fact Sheet 2014–3083, USGS Earthquake Science Center, May 2014.

[17] K. Faber and P. W. Maxwell, *Geophone spurious frequency: What is it and how does it affect seismic data?*, 2005, pp. 79–80. [Online]. Available: https://library.seg.org/doi/abs/10.1190/1.1826773

[18] M. Peter and M. Lansley, "What receivers will we use for low frequencies?" in *Proceedings of the SEG San Antonio Annual Meeting*, 2011, pp. 72–76.

[19] M. Casoni, C. Grazia, M. Klapez, N. Patriciello, A. Amditis, and E. Sdongos, "Integration of satellite and LTE for disaster recovery," *Communications Magazine, IEEE*, vol. 53, no. 3, pp. 47–53, March 2015.

[20] C. A. Grazia, M. Klapez, N. Patriciello, M. Casoni, A. Amditis, E. Sdongos, H. Gierszal, D. Kanakidis, C. Katsigiannis, K. Romanowski, P. Simplício, A. Oliveira, S. Sonander, and J. Jackson, "Integration between terrestrial and satellite networks: the PPDR-TC vision," in *2014 IEEE 10th International Conference on Wireless and Mobile Computing, Networking and Communications (WiMob)*, Oct 2014, pp. 77–84.

[21] M. Klapez, C. A. Grazia, and M. Casoni, "Towards massively multipath transmissions for public safety communications," in *2016 IEEE 12th International Conference on Wireless and Mobile Computing, Networking and Communications (WiMob)*, Oct 2016, pp. 1–7.

[22] M. Casoni, C. A. Grazia, and M. Klapez, "A software-defined 5G cellular network with links virtually pooled for public safety operators," *Transactions on Emerging Telecommunications Technologies*, vol. 28, no. 3, p. e3092, e3092 ett.3092.

[23] C. A. Grazia, M. Klapez, N. Patriciello, and M. Casoni, "Pink: Proactive injection into ack, a queue manager to impose fair resource allocation among tcp flows," in *2015 IEEE 11th International Conference on Wireless and Mobile Computing, Networking and Communications (WiMob)*, Oct 2015, pp. 132–137.

[24] D. Giardini, G. Grünthal, K. M. Shedlock, and P. Zhang, "The gshap global seismic hazard map," *Annals of Geophysics*, vol. 42, no. 6, 1999. [Online]. Available: https://www.annalsofgeophysics.eu/index.php/annals/article/view/3784

[25] A. L., F. M. Berardi, Bernardini, B. Brizuela, C. Caracciolo, C. Castellano, V. Castelli, A. Cavaliere, S. Del Mese, E. Ercolani, L. Graziani, A. Maramai, A. Massucci, A. Rossi, M. Sbarra, A. Tertulliani, M. Vecchi, and S. Vecchi, "Rapporto macrosismico sui terremoti del 20 (ML 5.9) e del 29 MAGGIO 2012 (ML 5.8 E 5.3) nella pianura padano-emiliana," Official Report, INGV - Istituto Nazionale di Geofisica e Vulcanologia, July 2012. [Online]. Available: http://terremoti.ingv.it/images/pdf/QUEST_Emilia2012_RapportoFinale.pdf

[26] O. Coussy and B. Zinszner, *Acoustics of porous media*. Editions Technip, 1987.